멤브레인(Membrane Journal)
Vol.13, No.1 March, 2003, 37-46

하전된 멤브레인 미세기공에서의 계면동전기적 유동에 의한 흐름전위: 비선형 Poisson-Boltzmann 전기장을 갖는 경우

전 명 석†

한국과학기술연구원 복잡유체 및 멤브레인 연구팀
(2003년 2월 11일 접수, 2003년 3월 5일 채택)

Electrokinetically Flow-Induced Streaming Potential Across the Charged Membrane Micropores: for the Case of Nonlinear Poisson-Boltzmann Electric Field

Myung-Suk Chun†

Complex Fluids and Membrane Team, Korea Institute of Science and Technology(KIST), Cheongryang, Seoul 130-650, KOREA
(Received February 11, 2003, Accepted March 5, 2003)

요 약: 하전된 멤브레인 미세기공으로 유체가 흐르는 경우는 계면동전기 효과가 작용하게 된다. 비선형 Poisson-Boltzmann 전기장과 흐름에 의해 유발되는 전기장 사이의 정전상호작용을 운동방정식의 외부작용 힘으로 고려하였다. 유한차분법으로 정전위 분포를 우선 산출하고, 이어서 Green 함수로 슬릿형 기공에 대한 Navier-Stokes 식의 해석해를 구하였다. 계면동전기적 유동에 의한 흐름전위를 관련된 물리화학적 인자들의 함수로 유도되는 해석적인 명확한 표현으로 제시하였다. 전기이중층, 표면전위, 그리고 기공벽면의 하전조건의 영향에 따른 유속분포와 흐름전위 변화를 고찰하였다. 계산결과, 전기이중층 두께나 표면전위가 증가함에 따라 평균유속은 감소하는 반면에 흐름전위는 증가하였다.

Abstract: The electrokinetic effect can be found in cases of the fluid flowing across the charged membrane micropores. The externally applied body force originated from the electrostatic interaction between the nonlinear Poisson-Boltzmann field and the flow-induced electrical field is taken into the equation of motion. The electrostatic potential profile is computed *a priori* by applying the finite difference scheme, and an analytical solution to the Navier-Stokes equation of motion for slit-like pore is obtained *via* the Green's function. An explicit analytical expression for the flow-induced streaming potential is derived as functions of relevant physicochemical parameters. The influences of the electric double layer, the surface potential of the wall, and the charge condition of the pore wall upon the velocity profile as well as the streaming potential are examined. With increasing of either the electric double layer thickness or the surface potential, the average fluid velocity is entirely reduced, while the streaming potential increases.

Keywords: *streaming potential, electrokinetic flow, electrostatic interaction, membrane pore, Poisson-Boltzmann equation*

1. Introduction

Since the late 1980s, numerous researchers regarding the membrane science have investigated on the determination of membrane electrokinetic properties by utilizing the Helmholtz-Smoluchowski equation [1-9]. The charge characterization of filtration membranes was recognized with the results being expressed in terms of membrane zeta potential [1-9].

As illustrated in Fig. 1, when a fluid is forced through a microchannel of membrane pore under an applied pressure, the counter-ions in the mobile part of

†Corresponding author (e-mail : mschun@kist.re.kr)

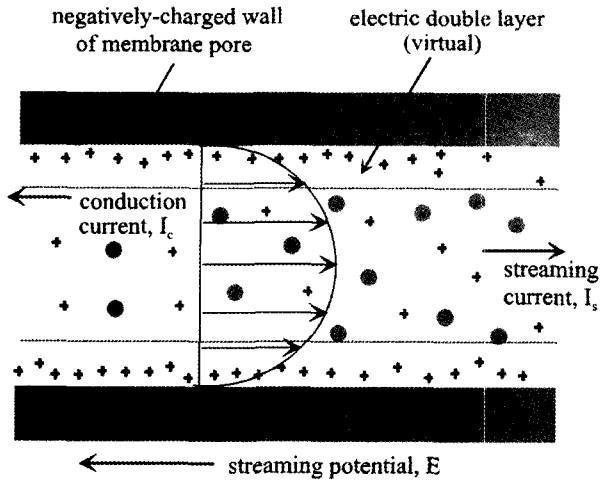

Fig. 1. Schematic view of a development of flow-induced streaming potential across a membrane pore filled with electrolyte aqueous solution, where the pore walls are same charged with constant surface potential.

the electric double layer (EDL) are carried toward the downstream end. Then an electric current called the streaming current results in the pressure-driven flow direction. Corresponding to this streaming current, there is an electrokinetic potential called the streaming potential. This flow-induced streaming potential acts to drive the counter-ions in the mobile part of the EDL to move in the direction opposite to the streaming current. This flow of ions in the opposite direction to the pressure-driven flow will generate conduction current. The overall result is a reduced flow rate in the direction of pressure drop. If the reduced flow rate is compared with the flow rate of uncharged inert case, it seems that the fluid would have a higher viscosity, which is usually referred to as the electroviscous effect. The effect of EDL is neglected, as the EDL thickness is quite small compared with the characteristic size of the flow channel. However, the EDL effect cannot be neglected in the filtrations with porous membranes, where the EDL thickness is comparable with the characteristic size of the pore.

Besides the microspace of membrane pore, microflows are important in the design and utilization of microfluidic devices, such as biomedical microchips and other MEMS (micro-electro mechanical system) devices [10]. Fluid flowing in microchannels with dimensions less than the order of tens of micrometers at readily achievable laminar flow speeds are characterized by low Reynolds number. The fluid flow in charged microchannels is definitely influenced by the electrokinetic effect and hence deviates from that described by the traditional form of the Navier-Stokes equation.

About forty years ago, the effect of the surface potential on fluid transport through narrow cylindrical capillary with the Debye-Hückel approximation was examined [11]. Later, the same problem with higher surface potential was investigated by developing an approximate solution to the Poisson-Boltzmann (P-B) equation pertaining to an imposed electric field [12]. In recent, the electrokinetic flow velocity in rectangular channels was estimated by solving coupled equation of motion with P-B equation [13]. For slit-like microchannel with a linearized P-B field, analytical solutions to the flow velocity and the flow-induced streaming potential have been obtained by employing the Green's function [14].

Based on the previous study, the electrokinetically flow-induced streaming potential in a well-defined slit-like membrane pore is analyzed here, by applying the Green's function formulation. The electrostatic potential is firstly considered by solving the nonlinear P-B equation using the finite difference method (FDM), and then the equation of motion is developed by dealing with the external body force. The electric potential profile is predicted with variations of ionic concentration of solution, surface potential, and charge condition of the pore wall, from which both the velocity profile and the streaming potential are estimated.

2. Explicit Analysis on Electrokinetic Flow Fields

2.1. Flow Through a Charged Slit-like Membrane Pore

The Navier-Stokes equation furnishes the paradigm

for describing the equation of motion for an incompressible ionic fluid, given by

$$\rho\frac{\partial \boldsymbol{v}}{\partial t} + \rho(\boldsymbol{v}\cdot\nabla)\boldsymbol{v} = -\nabla p + \boldsymbol{F} + \eta\nabla^2\boldsymbol{v} \quad (1)$$

where ρ and η are the density and viscosity of the fluid, respectively. For one-dimensional laminar flow through a slit-like pore, $\mathbf{v} = [0, 0, v_z(y)]$ is taken with Cartesian coordinates [15]. Neglecting gravitational forces, the body force per unit volume F ubiquitously caused by the z-directional action of an induced electrical field E_z on the net charge density ρ_e can be written $F_z = \rho_e E_z$. With these identities, Equation (1) is reduced to

$$\eta\frac{d^2v}{dy^2} = \frac{dp}{dz} + \rho_e E_z \ . \quad (2)$$

In view of taking a flow only in the z-direction in a slit spaced a distance 2H apart, the velocity profile v_z is known as a plane Poiseuille flow. One obtains the nondimensionalized equation of motion, such that

$$\frac{d^2V}{dY^2} = \frac{dP}{dZ} + \Gamma_1 E\sinh\Psi \quad (3)$$

with the following dimensionless parameters

$$Y = \frac{y}{d_h}\ ,\quad Z = \frac{z}{d_h Re}\ ,\quad V = \frac{v}{U}\ ,$$
$$Re = \frac{\rho d_h U}{\eta}\ ,\quad P = \frac{p}{\rho U^2}\ ,\quad E = \frac{E_z d_h Re}{\psi_o}\ ,$$
$$\Gamma_1 = \frac{2z_i e n_b \psi_o}{\rho U^2} \quad (4)$$

where d_h means the hydraulic diameter (i.e., 4H), U the reference velocity, and ψ_o the reference electrical potential. The boundary conditions are applied as

$$V = 0 \quad at\ \ Y = \frac{H}{d_h}\ , \quad (5a)$$

$$\frac{dV}{dY} = 0 \quad at\ \ Y = 0\ . \quad (5b)$$

Applying the Green's function reported in the previous study [14] can provide the velocity profile as follows (cf., for more detail, see Appendix A)

$$V(Y) = V_{inert}(Y) - \frac{d_h}{H}\sum_{n=1}^{\infty}\left(\frac{\cos\sqrt{\beta_n}Y}{\beta_n}\right)E\Gamma_1 \times\int_{-H/d_h}^{H/d_h} dY'\cos\sqrt{\beta_n}Y'\sinh\Psi\ . \quad (6)$$

Here, V_{inert} is the velocity profile in the absence of the electrostatic interaction, that equals to the plane Poiseuille flow profile as $(H^2/2\eta)(dp/dz)[1-(y/H)^2]$. Ultimately, the average fluid velocity is obtained as

$$\langle V\rangle = \frac{\int_0^{H/d_h} dY\,V}{\int_0^{H/d_h} dY}$$
$$= -\langle V\rangle_{inert} + \frac{d_h^2}{H^2}E\Gamma_1\sum_{n=1}^{\infty}\frac{(-1)^n}{\beta_n^{3/2}} \times\int_{-H/d_h}^{H/d_h} dY'\cos\sqrt{\beta_n}Y'\sinh\Psi$$
$$= -\frac{2d_h^2}{H^2}\sum_{n=1}^{\infty}\frac{1}{\beta_n^2}\frac{dP}{dZ} + \frac{d_h^2}{H^2}E\Gamma_1\sum_{n=1}^{\infty}\frac{(-1)^n}{\beta_n^{3/2}} \times\int_{-H/d_h}^{H/d_h} dY'\cos\sqrt{\beta_n}Y'\sinh\Psi\ . \quad (7)$$

2.2. Flow-induced electrokinetic potential or streaming potential

As derived in Equation (3), both the local and the average fluid velocities can be calculated when the nondimensional induced electrical field E is known. Ions from the double layer region are transported along with the solution, resulting in a streaming current I_s, in the direction of flow. The resultant induced electrokinetic potential, or the streaming potential E_z, then induces a flow of ions in the opposite direction known as the electrical conduction current I_c. Once the flow reaches a steady state, a summation of the streaming and the conduction currents should be zero, so that

$$\nabla\cdot I = I_s + I_c \equiv 0\ . \quad (8)$$

The streaming current I_s caused by the pressure-

driven flow is called the electrical convection current. For a slit-like micropore with the specified width W, it is defined by

$$I_s = Wd_h U \int dY \rho_e V \ . \tag{9}$$

The electrical conduction current I_c can be expressed as

$$I_c = \lambda_t E_z (2HW) = \lambda_t \frac{E\psi_o}{d_h Re} (2HW) \tag{10}$$

where λ_t is the total electrical conductivity and 2HW is the cross-sectional area of the pore. The electrical conduction current consists of bulk electrical conductivity and surface electrical conductivity. The bulk conductivity of the monovalent symmetric electrolyte (e.g., NaCl or KCl solution) is almost much greater than the surface conductivity of the pore wall made on inorganic or polymeric materials. In this respect, λ_t can be determined by the value of bulk conductivity alone.

Substituting Equations (9) and (10) into Equation (8), the nondimensional induced electrokinetic potential E is readily derived as

$$E = \frac{2d_h^2 \varepsilon \kappa^2 U}{H} \int_{-H/d_h}^{H/d_h} dY \sinh\Psi \left(\sum_{n=1}^{\infty} \frac{\cos\sqrt{\beta_n} Y}{\beta_n^{3/2}} (-1)^n \frac{dP}{dZ} \right) \Big/ \left[\frac{2H\psi_o \lambda_t}{d_h^2 Re} + \frac{d_h U \varepsilon \kappa^2 \Gamma_1}{H} \times \int_{-H/d_h}^{H/d_h} dY \sinh\Psi \left(\sum_{n=1}^{\infty} \frac{\cos\sqrt{\beta_n} Y}{\beta_n} \int_{-H/d_h}^{H/d_h} dY' \cos\sqrt{\beta_n} Y' \sinh\Psi \right) \right]$$
$$= \frac{d_h^2 \Gamma_2 Re}{H^2} \int_{-H/d_h}^{H/d_h} dY \sinh\Psi \left(\sum_{n=1}^{\infty} \frac{\cos\sqrt{\beta_n} Y}{\beta_n^{3/2}} (-1)^n \frac{dP}{dZ} \right) \Big/ \left[1 + \frac{d_h^2 \Gamma_1 \Gamma_2 Re}{2H^2} \times \int_{-H/d_h}^{H/d_h} dY \sinh\Psi \left(\sum_{n=1}^{\infty} \frac{\cos\sqrt{\beta_n} Y}{\beta_n} \int_{-H/d_h}^{H/d_h} dY' \cos\sqrt{\beta_n} Y' \sinh\Psi \right) \right] \tag{11}$$

where the dimensionless variable $\Gamma_2 = 2z_i e n_b d_h U / \lambda_t \psi_o$.

3. Long-Range Interaction with Nonlinear Poisson-Boltzmann Electric Field

For the charged surface contacting with electrolytes, the electrostatic charge would influence the distribution of nearby ions so that an electric field is established. The charges on the solid surface and the balancing charges in the liquid consist of both the compact double layer referred to as the Stern layer and the diffuse layer [16]. In order to compute the velocity profile and the streaming potential in a microchannel, the electric potential should be evaluated. A slit-like pore is confined between parallel planes of width 2H, then dimensionless nonlinear P-B equation governing the electric field leads to

$$\frac{\partial^2 \Psi}{\partial Y^2} = (\kappa d_h)^2 \sinh\Psi \ . \tag{12}$$

Here, the dimensionless potential Ψ denotes $z_i e\phi/kT$ and the inverse Debye length (i.e., inverse EDL thickness) κ is defined by

$$\kappa = \left[\frac{2n_{i,b} z_i^2 e^2}{\varepsilon kT} \right]^{1/2} \tag{13}$$

where z_i is the valence of type i ions, e the elementary charge, ε the dielectric constant, and kT the Boltzmann thermal energy. In Equation (13), $n_{i,b}$ is the concentration of type i ions in the bulk solution, where $n_{i,b}$ ($1/m^3$) equals to a product of Avogadro's number and ionic strength C_b(mM). For low potential of $\Psi \leq 1$ (i.e., less than kT/e = 25.69 mV) with 1:1 electrolyte, the P-B equation may be linearized. This linearized version is well-known as the Debye-Hückel equation.

Following boundary conditions are presented in a half of the slit cross-section,

$$\Psi = \Psi_s \quad at \quad Y = 0 \quad \text{and} \quad \frac{H}{d_h} \ . \tag{14}$$

Once the electric potential profile Ψ(Y) is obtained by applying the FDM provided in Appendix B, it is

straightforward to determine the local net charge density as follows

$$\rho_e = z_i e(n_+ - n_-) = -2z_i e n_{i,b} \sinh \Psi \quad . \quad (15)$$

4. Computational Practice

For illustrative computations, let us consider a laminar flow of an aqueous NaCl solution through a slit-like micropore of inorganic membrane. The half pore width H is virtually chosen to be 1 μm. The ionic concentration of 1:1 type electrolyte equals to the ionic strength of the solution. At room temperature, the dielectric constant ε and the viscosity η of the fluid are taken as $80\times(8.854\times10^{-12})$ Coul/N · m^2 and 1.0×10^{-3} kg/m · sec, respectively. The bulk conductivity with variations of ionic concentrations is chosen from the literature value [17], as given in Table 1. The finite difference grids of 1200 are built within the pore, and the convergence criterion is given as 10^{-5}. All computations performed on an IBM PC with Pentium IV processor (1.5 GHz) take less than 2 min.

The inner surfaces of micropore wall have surface potentials of both Ψ_s and $\widehat{\Psi_s}$. It can be assumed here that the surface potential is identical to the zeta potential. A decrease of NaCl electrolyte concentration C_b corresponds to an increase of Debye length κ^{-1}, which provides a measure of the range of long-range electrostatic interactions. The EDL thickness κ^{-1}(nm) equals to $[C_b(M)]^{-1/2}/3.278$ for 1:1 type electrolytes.

5. Results

The results of the potential profile can be seen in

Table 1. The Condition of NaCl Aqueous Solution Environment

Ionic strength, Cb (mM)	EDL thickness, κ^{-1} (nm)	Bulk conductivity ($1/\Omega$ · m)
1.0	9.7	1.2×10^{-2}
10^{-1}	30.5	1.4×10^{-3}
10^{-2}	96.5	1.6×10^{-4}
10^{-3}	305	1.7×10^{-5}

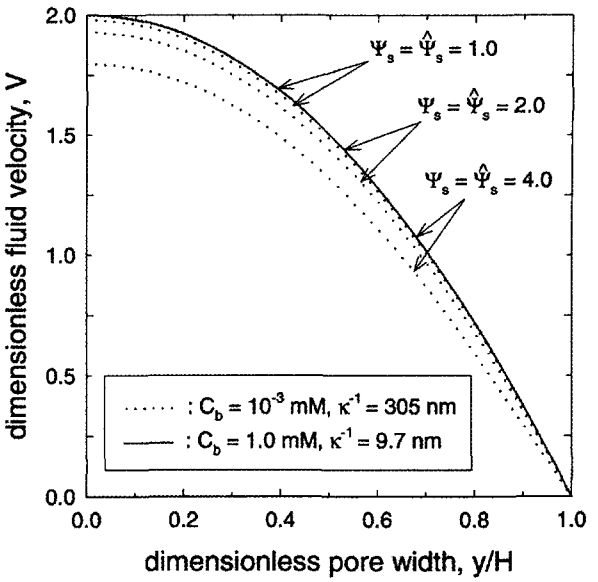

Fig. 2. Velocity profile in a same charged slit-like micropore for several solution ionic concentrations (i.e., Debye length) as well as surface potentials, where C_b = 10^{-3} mM and pressure gradient dp/dz is 1.0105 N/m^3.

the previous study [14], where it moves toward the center region as the surface potential increases. Getting far from the surface of the pore wall, the potential is decreased. An increase in the long-range repulsive screened electrostatic interaction with increasing the surface potential is more dramatic for lower solution ionic strength. Given the potential profile, the velocity profile V(Y) can subsequently be computed by using Equation (6). The flow situations are verified as a low Reynolds number condition, that is certainly less than 1. In Fig. 2., the EDL does not exhibit any effects on the flow pattern for the solution ionic strength of 1.0 mM. However, a dependency of the surface potential upon the velocity profile can distinctly be seen for the solution ionic strength of 10^{-3} mM. The average fluid velocity <v> is entirely reduced with the increase in surface potential as well as the decrease in solution ionic strength.

The charge condition of the wall surfaces also affects the velocity profile as given in Fig. 3, owing to the change of potential profiles. When each of the wall surfaces has opposite charge, the electrostatic attraction is experienced. As the electrostatic attraction increases,

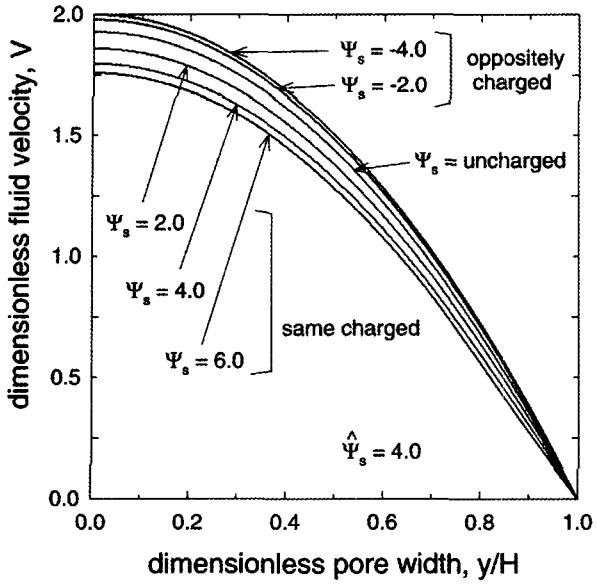

Fig. 3. Velocity profile in both same and oppositely charged slit-like micropores for several solution ionic concentrations (i.e., Debye length) as well as surface potentials, where C_b = 10^{-3} mM and pressure gradient dp/dz is 1.0105 N/m^3.

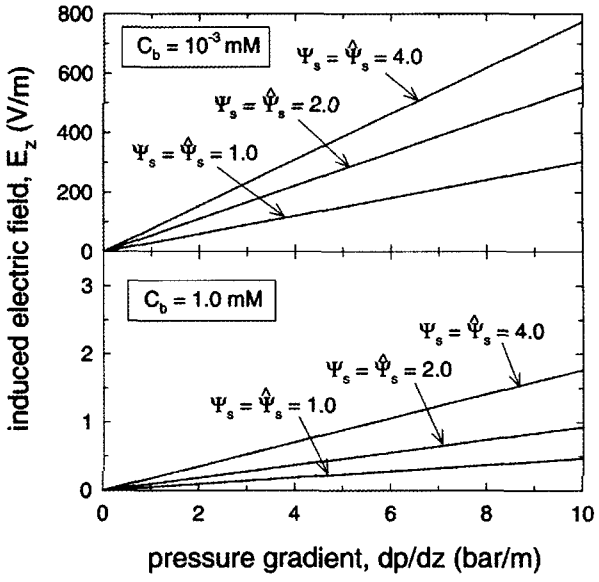

Fig. 4. The variations of induced electrical field E_z with pressure gradient at different solution ionic concentrations as well as surface potentials, where the slit walls have same charge.

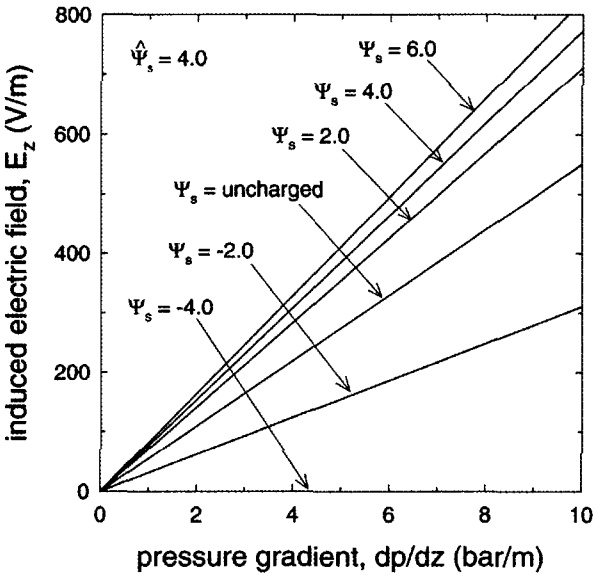

Fig. 5. The variations of induced electrical field E_z with pressure gradient at different solution ionic concentrations as well as surface potentials, where the slit walls have both same and opposite charges and C_b = 10^{-3} mM.

the maximum velocity in the center of the pore is increased. Once each of the wall surfaces has opposite charge with equivalent magnitude of the potential, then the velocity profile becomes the Poiseuille flow.

As described before, the charge concentration difference between the upstream and the downstream results in an induced electrokinetic potential, namely streaming potential. Therefore, a larger pressure gradient will generate a larger volume transport, a higher charge accumulation as well as a stronger induced electrical field will occur. In Fig. 4, the induced electrical field increases as the surface potential increases for the given pressure gradient. Also, the induced electrical field increases with the decrease in solution ionic strength, due to a larger EDL thickness. This behavior leads us to understand the electrokinetic effect on the fluid velocity. In Fig. 5, the opposite charge generates the opposite streaming current, which would decrease the net streaming current through the pore, resulting reduction of the streaming potential. This is due to a fact that the fluid velocity increases favorably in accordance with increasing of the effect of opposite charge, as shown in Fig. 3.

Since the electroviscous effect results from the moving ions in the diffuse layer, the viscosity

enhancement becomes stronger with the increases of the Debye length (i.e., a decrease of the solution ionic strength) as well as the surface potential. The electroviscous effect becomes weakened for the case of oppositely charged wall. A reduction of the conduction current due to the opposite charge gives rise to a decrease in the electroviscous effect.

6. Conclusions

A micropore analysis of the requisite membrane characterization problems has been usefully confronted. The main thrust of the present study is an analysis on the electrokinetically flow-induced streaming potential across slit-like micropores. The additional body force originated from the presence of the nonlinear P-B electric field and the flow-induced electrical field was considered in the equation of motion. Applying the Green's function formula could derive the expressions in explicit forms for the velocity profile and the streaming potential as functions of relevant parameters.

Theoretical results emphasize that the velocity profile is clearly affected by the EDL for the cases of low ionic concentrations and high surface potentials, where the average fluid velocity decreases as the solution ionic concentration decreases. Since both the EDL and the induced electrokinetic potential act against the liquid flow, they result in an enhanced streaming potential. This study explored the influence of the surface charge condition upon both the velocity profile and the streaming potential. Compared to the case of same charge, the pore walls of opposite charge display an opposite behavior on the average fluid velocity as well as the streaming potential.

Appendix A: The Velocity Profile by Green's Function Formulation

The Green's function G with the differential operator L can be devoted to V(Y,t) as follows

$$LV = \left[\eta\frac{\partial}{\partial t} - \frac{\partial^2}{\partial Y^2}\right]V = -\frac{\partial P}{\partial V} - E\Gamma_1 \sinh\Psi(Y) \ . \quad \text{(A1)}$$

Proceeding by standard techniques, we consider the Green's function as a linear combination of eigenvalues and corresponding eigenfunctions Φ_n, established as

$$G(Y, Y', t) = \sum_n^{\infty} e^{-\beta_n t}\Phi_n(Y)\Phi_m(Y') \quad \text{(A2)}$$

where t is normalized by $\rho d_h^2/\eta$, and a convenient representation for the eigenvalues $\beta_n = [(2n\text{-}1)\pi d_h/2H]^2$. Utilization of the Dirac delta function with orthogonal properties leads to the following expression

$$LG(Y, Y', t) \equiv \delta(Y - Y')\delta(t) \ . \quad \text{(A3)}$$

Then, a solution of Equation (A1) subjecting to the boundary conditions is given by

$$V(Y, t) = \int_0^t dt' \int_0^{H/d_h} dY' G(Y, Y', t-t') \times \left[-\frac{dP}{dZ} - E\Gamma_1 \sinh\Psi(Y')\right] \ . \quad \text{(A4)}$$

The Green's function is explicitly found by using the separation of variables method, yielding

$$G = \frac{d_h}{H}\sum_{n=1}^{\infty} e^{-\frac{(2n-1)^2\pi^2 d_h^2}{4H^2}t} \times \cos\frac{(2n-1)\pi d_h}{2H}Y \cos\frac{(2n-1)\pi d_h}{2H}Y' \ . \quad \text{(A5)}$$

A proper solution for velocity profile yields as

$$V(Y, t) = \frac{d_h}{H}\sum_{n=1}^{\infty}\lim_{t\to\infty}\int_0^t dt' \ e^{-\beta_n(t-t')} \times \int_{-H/d_h}^{H/d_h} dY' \cos\sqrt{\beta_n}Y \cos\sqrt{\beta_n}Y' \times \left[-\frac{dP}{dZ} - E\Gamma_1 \sinh\Psi(Y')\right] \ . \quad \text{(A6)}$$

Both integrating and rearranging give the velocity profile as follows,

$$V(Y) = \frac{2d_h}{H}\sum_{n=1}^{\infty}\left(\frac{\cos\sqrt{\beta_n}Y}{\beta_n}\right) \times\left[\frac{(-1)^n}{\sqrt{\beta_n}}\frac{dP}{dZ} - \frac{E\Gamma_1}{2}\int_{-H/d_h}^{H/d_h} dY'\cos\sqrt{\beta_n}Y'\sinh\Psi\right] \quad (A7)$$

which means Equation (6).

Appendix B: Electric Potential by Finite Difference Scheme

To obtain the solution of Equation (12), taking five-point central difference method yields the left-hand side of Equation (12) as

$$\frac{\partial^2\Psi}{\partial Y^2} = \frac{\Psi_{j+1}^{k+1} - 2\Psi_j^{k+1} + \Psi_{j-1}^{k+1}}{(\Delta Y)^2} \quad (B1)$$

where k means the iteration index and the grid index j = 1, 2, ... , N. The *ansatz* functions on the right-hand side of Eq. (12) can be linearized as

$$\sinh\Psi_j^k = \sinh\Psi_j^k + (\Psi_j^{k+1} - \Psi_j^k)\cosh\Psi_j^k \ . \quad (B2)$$

Substituting Equations. (B1) and (B2) into Equation (12), the finite difference form of the nonlinear P-B equation becomes as

$$\frac{\Psi_{j+1}^{k+1} - 2\Psi_j^{k+1} + \Psi_{j-1}^{k+1}}{(\Delta Y)^2} = \kappa^2[\sinh\Psi_j^k + (\Psi_j^{k+1} - \Psi_j^k)\cosh\Psi_j^k] \ . \quad (B3)$$

Then,

$$\Psi_{j+1}^{k+1} - (2 + (\Delta Y)^2\kappa^2\cosh\Psi_j^k)\Psi_j^{k+1} + \Psi_{j-1}^{k+1} = (\Delta Y)^2\kappa^2(\sinh\Psi_j^k - \Psi_j^k\cosh\Psi_j^k) \ . \quad (B4)$$

Equation (B4) can be solved for Ψ_j^{k+1} by successive iterative calculation, using the value of Ψ obtained in the k-th iteration [18]. A series of algebraic equations can be expressed as a matrix form, given by

$$\boldsymbol{A}\cdot\boldsymbol{x} = \boldsymbol{b} \quad (B5)$$

where

$$\boldsymbol{x}^T = [\Psi_1^{k+1}, \Psi_2^{k+1}, \ldots \Psi_j^{k+1}, \ldots \Psi_{N-1}^{k+1}, \Psi_N^{k+1}] \quad (B6)$$

$$\boldsymbol{b}^T = [Q(\Psi_1^k) - \Psi_s, Q(\Psi_2^k), \ldots Q(\Psi_j^k), \ldots Q(\Psi_{N-1}^k), Q(\Psi_N^k) - \Psi_s] \quad (B7)$$

$$\boldsymbol{A} = \begin{bmatrix} M(\Psi_1^k) & 1 & 0 & \cdots & \cdots & 0 \\ 1 & M(\Psi_2^k) & 1 & & \iddots & \vdots \\ 0 & 1 & \ddots & \ddots & & \vdots \\ \vdots & & \ddots & \ddots & 1 & 0 \\ \vdots & \iddots & & 1 & M(\Psi_{N-1}^k) & 1 \\ 0 & \cdots & \cdots & 0 & 1 & M(\Psi_N^k) \end{bmatrix} \quad (B8)$$

In Equations (B7) and (B8), the constant potential boundary condition takes as $M(\Psi) = -2 - (\Delta Y)^2\kappa^2\cosh\Psi$ and $Q(\Psi) = (\Delta Y)^2\kappa^2(\sinh\Psi - \Psi\cosh\Psi)$.

Acknowledgement

This work was supported by grant No. R01-2001-000-00411-0 from the Korea Science and Engineering Foundations and the research fund of the KIST (2E17460).

Nomenclature

C_b : solution ionic strength [M]
d_h : hydraulic diameter [m]
E : dimensionless induced electrokinetic potential, or streaming potential [-]

E_z : dimensional E [V/m]
e : elementary charge [Coul]
F : body force [N/m^3]
H : half pore width [m]
I : net electrical current [A]
I_c : electrical conduction current [A]
I_s : electrical convection current [A]
kT : Boltzmann thermal energy [J]
$n_{i,b}$: concentration of charged ions [$1/m^3$]
P : dimensionless hydraulic pressure [-]
p : hydraulic pressure [N/m^2]
Re : Reynolds number [-]
t : dimensionless time [-]
U : reference velocity [m/s]
V : dimensionless fluid velocity [-]
<V> : dimensionless average fluid velocity [-]
v : fluid velocity component [m/s]
W : specified width [m]
Y : non-dimensional lateral (y-) coordinate [-]
Z : non-dimensional axial (z-) coordinate [-]
z_i : valence of ion [-]

Greek Letters

β_n : set of eigenvalues [-]
ε : dielectric constant [$Coul^2/J \cdot m$]
Φ_n : set of eigenfunctions [-]
κ : inverse Debye length, or inverse EDL thickness [1/m]
ρ : fluid density [kg/m^3]
ρ_e : net charge density [$Coul/m^3$]
η : fluid viscosity [$kg/m \cdot s$]
Γ_1, Γ_2 : non-dimensional parameters [-]
λ_t : total electrical conductivity [$1/\Omega \cdot m$]
Ψ : dimensionless electrostatic potential [-]
Ψ_s : dimensionless electrostatic surface potential [-]
$\widehat{\Psi_s}$: dimensionless electrostatic surface potential of opposing wall [-]
ψ_o : reference electrical potential [V]

Mathematical

A : finite difference matrix [-]
b : finite difference vector [-]
G : Green's function [-]
L : differential operator [-]
x : solution vector [-]
δ : Dirac delta function [-]

References

1. M. Nyström, M. Lindström, and E. Matthiasson, "Streaming potential as a tool in the characterization of ultrafiltration membranes", *Colloids Surfaces*, **36**, 297 (1989).
2. C. Causserand, M. Nyström, and P. Aimar, "Study of streaming potentials of clean and fouled ultrafiltration membranes", *J. Membrane Sci.*, **88**, 211 (1994).
3. K. J. Kim, A. G. Fane, M. Nyström, A. Pihlajamäki, W. R. Bowen, and H. Mukhtar, "Evaluation of electroosmosis and streaming potential for measurement of electric charges of polymeric membranes", *J. Membrane Sci.*, **116**, 149 (1996).
4. W. R. Bowen and X. Cao, "Electrokinetic effects in membrane pores and the determination of zeta-potential", *J. Membrane Sci.*, **140**, 267 (1998).
5. A. Szymczyk, P. Fievet, M. Mullet, J. C. Reggiani, and J. Pagetti, "Comparison of two electrokinetic methods: electro-osmosis and streaming potential to determine the zeta-potential of plane ceramic membranes", *J. Membrane Sci.*, **143**, 293 (1998).
6. D. Möckel, E. Staude, M. Dal-Cin, K. Darcovich, and M. Guiver, "Tangential flow streaming potential measurements: Hydrodynamic cell characterization and zeta potentials of carboxylated polysulfone membranes", *J. Membrane Sci.*, **145**, 211 (1998).
7. P. Fievet, A. Szymczyk, B. Aoubiza, and J. Pagetti, "Evaluation of three methods for the characterization of the membrane-solution interface: streaming potential, membrane potential and electrolyte conductivity inside pores", *J. Membrane Sci.*, **168**, 87 (2000).
8. M.-S. Chun, H. I. Cho, and I. K. Song, "The

electrokinetic behavior of membrane zeta potential during the filtration of colloidal suspensions", *Desalination*, **148**, 363 (2002).
9. A. E. Yaroshchuk, Y. P. Boiko, and A. L. Makovetskiy, "Filtration Potential across Membranes Containing Selective Layers", *Langmuir*, **18**, 5154 (2002).
10. A. Manz, C. S. Effenhauser, N. Burggraf, D. J. Harrison, K. Seller, and K. Flurl, "Electroosmotic pumping and electrophoretic separations for miniaturized chemical analysis systems", *J. Micromech. Microeng.*, **4**, 257 (1994).
11. C. L. Rice and R. Whitehead, "Electrokinetic Flow in a Narrow Cylindrical Capillary", *J. Phys. Chem.*, **69**, 4017 (1965).
12. S. Levine, J. R. Marriott, G. Neale, and N. Epstein, "Theory of Electrokinetic Flow in Fine Cylindrical Capillaries at High Zeta-Potentials", *J. Colloid Interface Sci.*, **52**, 136 (1975).
13. D. Li, "Electro-viscous effects on pressure-driven liquid flow in microchannels", *Colloids Surfaces A*, **195**, 35 (2001).
14. M.-S. Chun, "Electrokinetic Flow Velocity in Charged Slit-like Microfluidic Channels with Linearized Poisson-Boltzmann Field", *Korean J. Chem. Eng.*, **19**, 729 (2002).
15. J. Happel and H. Brenner, "Low Reynolds number hydrodynamics: with special applications to particulate media", Martinus Nijhoff, Hague (1983).
16. R. J. Hunter, "Zeta Potential in Colloid Science: Principles and Applications", Academic Press, New York (1981).
17. D. R. Lide (Eds.), "CRC Handbook of Chemistry and Physics", 80th Ed., CRC Press, FL (1999).
18. C. F. Gerald and P. O. Wheatley, "Applied Numerical Analysis", 4th Ed., Addison-Wesley, Tokyo (1992).